Applied Geochemistry 24 (2009) 1270–1277

Contents lists available at ScienceDirect

Applied Geochemistry

journal homepage: www.elsevier.com/locate/apgeochem

# Application of iron and zinc isotopes to track the sources and mechanisms of metal loading in a mountain watershed

David M. Borrok [a,*], Richard B. Wanty [b], W. Ian Ridley [b], Paul J. Lamothe [b], Briant A. Kimball [c], Philip L. Verplanck [b], Robert L. Runkel [b]

[a] Department of Geological Sciences, University of Texas, El Paso, TX 79968, United States
[b] US Geological Survey, Denver Federal Center, Denver, CO 80225, United States
[c] US Geological Survey, 2329 W. Orton Cir., Salt Lake City, UT 84119, United States

ARTICLE INFO

*Article history:*
Received 26 August 2008
Accepted 27 March 2009
Available online 5 April 2009

Editorial handling by Dr. R. Fuge

ABSTRACT

Here the hydrogeochemical constraints of a tracer dilution study are combined with Fe and Zn isotopic measurements to pinpoint metal loading sources and attenuation mechanisms in an alpine watershed impacted by acid mine drainage. In the tested mountain catchment, $\delta^{56}$Fe and $\delta^{66}$Zn isotopic signatures of filtered stream water samples varied by ~3.5‰ and 0.4‰, respectively. The inherent differences in the aqueous geochemistry of Fe and Zn provided complimentary isotopic information. For example, variations in $\delta^{56}$Fe were linked to redox and precipitation reactions occurring in the stream, while changes in $\delta^{66}$Zn were indicative of conservative mixing of different Zn sources. Fen environments contributed distinctively light dissolved Fe (<−2.0‰) and isotopically heavy suspended Fe precipitates to the watershed, while Zn from the fen was isotopically heavy (>+0.4‰). Acidic drainage from mine wastes contributed heavier dissolved Fe (~+0.5‰) and lighter Zn (~+0.2‰) isotopes relative to the fen. Upwelling of Fe-rich groundwater near the mouth of the catchment was the major source of Fe ($\delta^{56}$Fe ~ 0‰) leaving the watershed in surface flow, while runoff from mining wastes was the major source of Zn. The results suggest that given a strong framework for interpretation, Fe and Zn isotopes are useful tools for identifying and tracking metal sources and attenuation mechanisms in mountain watersheds.

© 2009 Elsevier Ltd. All rights reserved.

## 1. Introduction

Mountain watersheds are critical components in the hydrologic cycle, capturing and storing enormous quantities of water that ultimately supply and/or recharge a large part of the available freshwater on Earth (e.g., Bales et al., 2006). Metal sulfide deposits are common in many mountain regions and are often associated with extensive zones of pyritic alteration that sometimes host economic quantities of base (e.g., Cu, Zn, and Pb) and/or precious (e.g., Au and Ag) metals. Oxidative weathering of these sulfide minerals in host rock with insufficient acid-neutralizing capacity generates acidic, metal-rich fluids that can impact water quality (e.g., Brooks et al., 2001; Kimball et al., 2002; Williams et al., 2002). Unfortunately, the processes governing the loading (or attenuation) of metals like Fe and Zn in mountain regions are poorly understood, because mountain catchments are difficult to access, surface and groundwater flow pathways are often ambiguous, and monitoring wells and other infrastructure are generally absent. These complications also make it difficult to distinguish between anthropogenic and natural sources of metal-loading despite the fact that this distinction is important for establishing realistic remediation strategies (e.g., Runkel and Kimball, 2002; Kimball et al., 2002; Wanty et al., 2004; Johnson and Hallberg, 2005).

Stable Fe and Zn isotopes have emerged as tools to examine the sources and mechanisms controlling the cycling of Fe and Zn in rivers and soils (e.g., Fantle and DePaolo, 2004; Emmanuel et al., 2005; Bergquist and Boyle, 2006; Ingri et al., 2006; Borrok et al., 2008a; Chen et al., 2008). Isotopes of Fe are fractionated by changes in redox state (e.g., Welch et al., 2003; Anbar et al., 2005), complexation with soil organic matter (Brantley et al., 2001), bacterial interactions (e.g., Crosby et al., 2007), and during surface adsorption and mineral precipitation reactions (e.g., Icopini et al., 2004; Skulan et al., 2002; Balci et al., 2006). Zinc is not a redox sensitive element under most natural conditions, and although non-redox fractionations attributable to processes like surface adsorption and complexation with natural organic matter are measurable (Pokrovsky et al., 2005; Balistrieri et al., 2008; Jouvin et al., submitted for publication), Zn often behaves conservatively in aqueous systems (e.g., Chen et al., 2008). Hence, Zn isotopes in fluids, soils, and sediments are thought to closely represent the Zn isotopic compositions of the original metal sources. Zinc isotopes have been adapted specifically to identify and track anthropogenic metal sources (e.g., Cloquet et al., 2006; Weiss et al., 2007; Chen et al., 2008; Sonke et al., 2008).

* Corresponding author. Tel.: +1 915 747 5850.
*E-mail address:* dborrok@utep.edu (D.M. Borrok).

0883-2927/$ - see front matter © 2009 Elsevier Ltd. All rights reserved.
doi:10.1016/j.apgeochem.2009.03.010

Because streams are integrators for geochemical processes on the catchment scale, Fe and Zn isotopes in stream waters may provide key insights into the relative contributions of different metal sources, and may be used as direct probes of the mechanisms controlling metal cycling. However, to accurately interpret Fe and Zn isotopic measurements in stream waters, it is necessary to build a quantitative hydrogeochemical framework for a given catchment. Tracer injection studies provide a method for providing such a framework by quantifying stream water discharge and inflow volumes through dilution calculations (Kimball et al., 2002, 2007). In this study a tracer dilution investigation is combined with traditional geochemical data and Fe and Zn isotopic measurements of stream water to pinpoint different anthropogenic and natural metal sources and to unravel the mechanisms responsible for metal attenuation in an alpine watershed.

## 2. Field setting

The investigation focuses on the Prospect Gulch (referred to herein as PG) alpine/sub-alpine catchment (~3000–3800 m in elevation) located in the Upper Animas River watershed within the San Juan Mountains, Colorado (Fig. 1). The region is dominated by volcanic and volcaniclastic sedimentary rocks that were emplaced during the formation of the San Juan caldera at about 28.2 Ma (Lipman et al., 1976; Bove et al., 2000). Mineralization in the area is characterized by widespread pyritization, particularly in the upper 2/3 of the watershed, and fault/vein controlled ore bodies consisting of Cu, Fe, Zn and Pb sulfides with substantial accessory concentrations of Au and Ag. Complete characterizations of the ore minerals and hydrothermal alteration zones are summarized in Bove et al. (2007). Numerous abandoned mines and shafts are scattered throughout the watershed, including the former Galena Queen, Lark, Henrietta, and Joe and Johns Mines, all of which are associated with sulfide-rich waste-rock piles. The PG watershed is ~5 $km^2$, and is drained by a ~2.5 km long stream that changes in elevation by ~800 m before emptying into Cement Creek. Field work was conducted in September, 2006, during base-flow conditions.

## 3. Materials and methods

The tracer injection procedure and load calculations are presented in Kimball et al. (2007) and Runkel et al. (2007) and are only summarized here. The purpose of the tracer injection was to quantify stream loads (i.e., the flux of stream flow multiplied by constituent concentrations) for Fe, Zn and other key elements in PG. A conservative LiBr tracer solution was continuously injected at a steady flow rate in the upper part of PG (Fig. 1). The tracer reached a steady-state over the first ~1700 m of the stream after 1.5 days, but was slowed by avalanche debris below this point. Dilution calculations downstream of this point were supplemented with a smaller-scale $Br^-$ slug tracer (near the mouth of the catchment), gauging measurements, and dilution information for natural tracers like Sr (i.e., Sr is believed to behave conservatively over this stretch of PG). Water samples were collected in the main stream channel and from all tributaries over an 8-h period either by hand

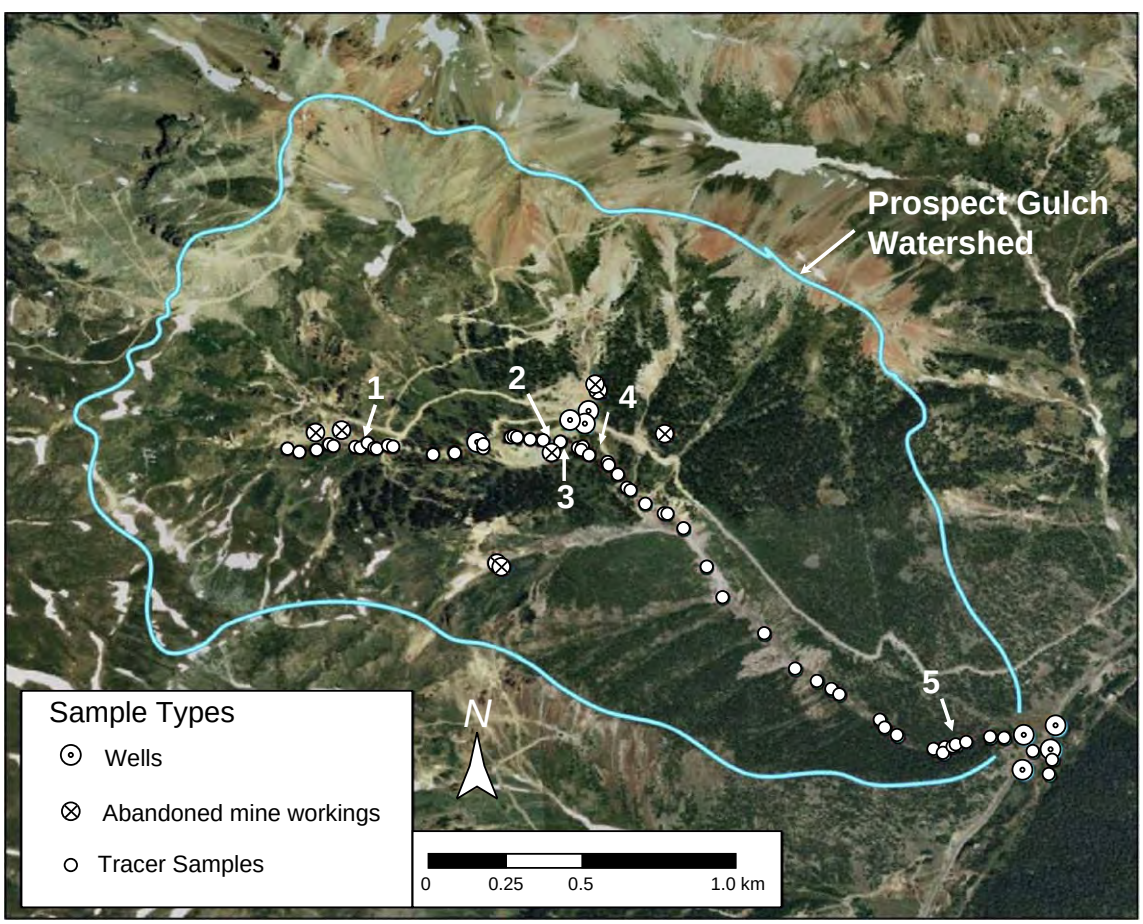


**Fig. 1.** Location map for Prospect Gulch watershed. Sample locations, well locations, and the sites of abandoned mine workings are depicted. Numbers 1–5 correspond to zones of metal loading that are discussed in the text.

or by automatic samplers. Because Li and Br generally behave conservatively in mountain streams, decreases in the concentrations of Li and Br downstream (until steady state was lost after ~1700 m) were attributed solely to dilution. Sample bottles (that were earlier acid-washed and rinsed three times with pure water) were transferred to an on-site field laboratory within 3 h where they were split into filtered (0.45-μm)-acidified, filtered-un-acidified, and unfiltered-acidified subsets. Selected samples were filtered to 0.001-μm using a tangential flow filter system. Water quality parameters, including pH, temperature and conductivity were measured at each sample location using a calibrated multiparameter instrument.

Water samples were also collected from a series of monitoring wells in the lower and middle reaches of the catchment (Fig. 1; well location and installation information are presented in Johnson and Yager, 2006). Wells were sampled with a peristaltic pump and clean plastic tubing. For deep wells, $N_2$ was used to provide pressure to drive water from depth to the surface via a specialized tubing assembly within the well (see Johnson and Yager, 2006). Well samples were processed identically to stream water samples. A representative quartz-sericite-pyrite (QSP)-altered volcanoclastic rock near the stream channel (~1000 m downstream) was additionally selected for bulk geochemical and isotopic analysis (see Fernandez and Borrok, 2009).

Total (unfiltered) metal, dissolved metal, and major cation concentrations for stream waters, well waters, and the digested rock sample were determined by inductively coupled plasma mass spectroscopy (ICP-MS; Lamothe et al., 2002). Iron(II) concentrations were determined by colorimetry and anions were measured by ion chromatography (Brinton et al., 1995). Field and trip blanks were absent of measurable Fe and Zn. Selected rock and water samples were prepared for isotopic analysis using an anion-exchange chromatography separation technique (Borrok et al., 2007). Isotopic analyses were performed at the USGS laboratories in Denver, Colorado using a Nu Instruments® MC-ICP-MS.

Samples were introduced to the Ar plasma via a Nu Instruments desolvating nebulizer system (DSN 100) at a fluid flow rate of 0.1 mL/min. Previous investigation of the Ni signal using $^{60}$Ni confirmed that the possible isobaric interference of $^{64}$Ni on $^{64}$Zn was insignificant under the operating conditions (Balistrieri et al., 2008; Borrok et al., 2008a). Wash out times between samples (2% $HNO_3$) were monitored and adjusted in real time to ensure that the signal returned to background levels prior to the next analysis. A 2% $HNO_3$ blank correction, measured for 60 s prior to each analysis was subtracted from the isotopic measurements of both samples and standards. Column procedural blanks were analyzed for each set of samples, and blank contributions were found to be negligible and did not require any data corrections. For Zn analysis, isotopes of masses 64, 66, and 68 were simultaneously measured. A Johnson Matthey Zn standard, batch JMC 3-0749-L, was used as a reference material and subjected to the same ion-exchange column procedure prior to measurement. Isotopic results are reported in standard delta notation (units of ‰) relative to the average of the bracketing standards:

$$\delta^{66}\mathrm{Zn} = \left[\frac{(^{66}\mathrm{Zn}/^{64}\mathrm{Zn})_{\mathrm{sample}}}{(^{66}\mathrm{Zn}/^{64}\mathrm{Zn})_{\mathrm{JMC_{ave}}}} - 1\right] \times 1000 \quad (1)$$

For Fe, isotopic masses of 54, 56, and 57 were simultaneously measured in pseudo-high resolution mode, to resolve $^{54}$Fe, $^{56}$Fe, and $^{57}$Fe peaks from their respective N- and O-argide interferences. Isotopic ratios are reported relative to the IRMM-14 reference material (also subjected to the column procedure):

$$\delta^{56}\mathrm{Fe} = \left[\frac{(^{56}\mathrm{Fe}/^{54}\mathrm{Fe})_{\mathrm{sample}}}{(^{56}\mathrm{Fe}/^{54}\mathrm{Fe})_{\mathrm{IRMM14}}} - 1\right] \times 1000 \quad (2)$$

The "standard-sample-standard" bracketing technique was used as the sole correction for drift and mass bias in both the Fe and Zn systems. The validity of this approach for samples introduced to the Nu Plasma instrument via the DSN 100 was confirmed through mass bias tests presented in Borrok et al. (2007), and was recently affirmed in a comprehensive study by Petit et al. (2008). Additional quality assurance checks included: (1) duplicate column separations to verify reproducibility, (2) independent assessment of the completeness of the column recovery (100 ± 6%), and (3) checking of the purity of the isotopic separates through analysis with a traditional ICP-MS. The average 2$\sigma$ uncertainty calculated from replicate measurements of unknowns (including column duplicates) over multiple analytical sessions was 0.07‰ for Zn and 0.2‰ for Fe. Plots of $\delta^{66}$Zn vs. $\delta^{68}$Zn and $\delta^{57}$Fe vs. $\delta^{56}$Fe reflected the appropriate mass dependence for each system ($\delta^{68}\mathrm{Zn} = 1.97 \times \delta^{66}\mathrm{Zn}$, $R^2 = 0.99$; $\delta^{57}\mathrm{Fe} = 1.47 \times \delta^{56}\mathrm{Fe}$, $R^2 = 0.99$, data not shown). Additional discussions of isotopic uncertainties are presented elsewhere (Borrok et al., 2007, 2008a; Balistrieri et al., 2008).

## 4. Results

Fig. 2 presents pH data for individual stream samples (38 total) and inflows to the main stream channel (28 total) that were collected during the LiBr tracer injection. Stream pH was circumneutral in the uppermost reaches of the watershed, but rapidly decreased to ~3.5 in response to the loading of protons from several acidic inflows around 1000 m downstream (Fig. 2). All stream, stream inflow, and well samples were analyzed for major and trace element concentrations and the data are presented in Table 1S in the online electronic data repository. For comparative purposes selected data are plotted in the form of $\log(C/C_i)$ in Fig. 3, where $C$ is the dissolved concentration of the measured trace (Fig. 3a) or major (Fig. 3b) element and $C_i$ is the initial dissolved concentration of that element in the upper part of the stream above the injection point. This plotting technique was adopted from Chapman et al. (1983) who used it to track metal attenuation in streams affected by acid mine drainage. Changes in $\log(C/C_i)$ over the 2.5 km length of the stream reflect either (1) dilution, (2) loading from source areas, or (3) in-stream geochemical processes. Fig. 4 presents the predicted speciation of Fe for each filtered stream sample calculated using PHREEQC (Parkhurst and Appelo, 1999). Input for the equilibrium modeling included the concentrations of all major

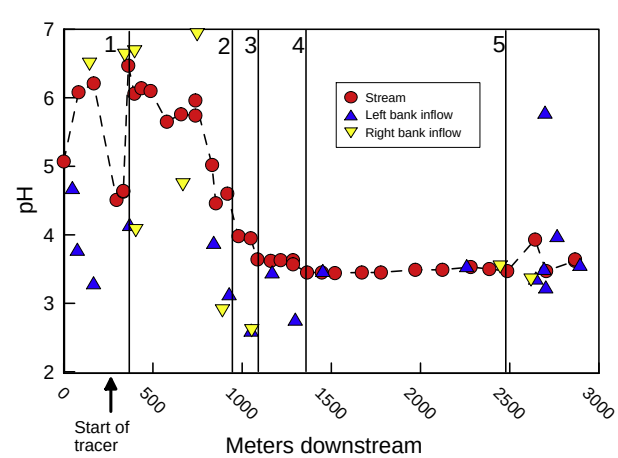


**Fig. 2.** The pH of stream and inflow samples in Prospect Gulch. Right and left bank inflows are oriented from the perspective of someone looking downstream. Numbers 1–5 and the associated lines denote locations of Fe or Zn loading discussed in the text.

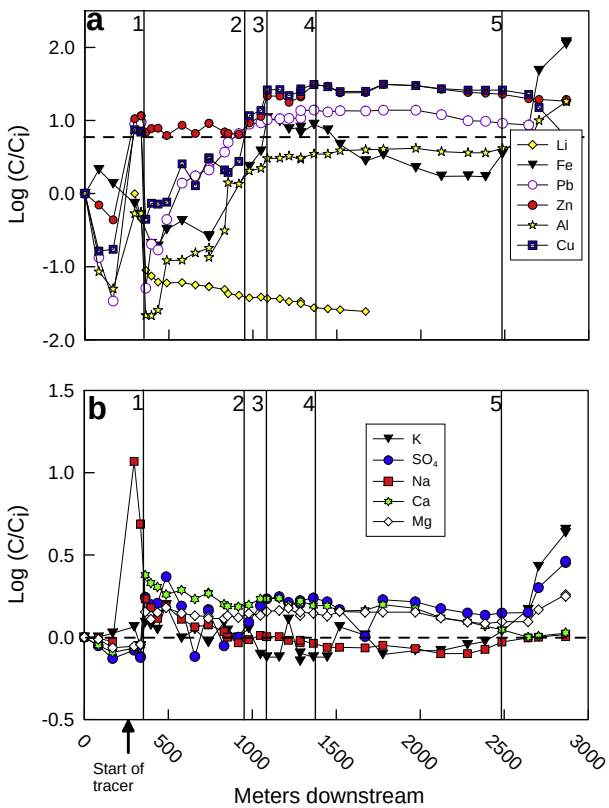


**Fig. 3.** Log($C/C_i$) of selected trace (A) and major (B) elements, including the Li tracer, where $C$ is the concentration of the dissolved element and $C_i$ is the concentration of the dissolved element at the most upstream point where the tracer was injected into the stream. A log ($C/C_i$) of 0 (dashed line) indicates no change in concentration relative to the starting point. Li data are not shown after 1671 m downstream because the tracer did not reach steady-state after this point and additional data (described in the text) were necessary to calculate dilution. Numbers 1–5 and the associated lines denote locations of Fe or Zn loading discussed in the text.

cations, anions, and trace metals (including individual Fe(II) and Fe(III) concentrations) for every stream sample. Modeling did not account for possible dissolved metal–organic complexes (TOC was not measured in the study) nor surface adsorption reactions (although the extent of adsorption was likely modest under the acidic pH conditions). Fig. 4 indicates that Fe(II) dominates in the upper and lower reaches of the stream, while a variety of Fe(III)-sulfate, and -hydroxide complexes are most abundant from ~1000 to 2400 m downstream (Fig. 4). Zinc species (not plotted) did not vary substantially and were dominated by $Zn^{+2}$ with lesser $ZnSO_4$.

Discharge for PG and the volume of flow for individual inflows into the main stream channel were calculated from LiBr tracer data (supplemented with the $Br^-$ slug tracer, gauging information, and Sr dilution data) using conservation of mass and flow equations described by Kimball et al. (2007). Flow rates ranged from 0.2L/s upstream near the start of the tracer to 16L/s at the mouth of PG. The calculated flow data for PG and all the inflows to PG are presented in Table 1S. Discharge data were combined with concentration data to calculate the mass load in kg/day for individual elements. Fig. 5 presents the dissolved (<0.45 μm), total (unfiltered), and cumulative instream Fe loads in PG (note the log scale for kg/day) and the Fe isotopic data for the measured stream and inflow samples. The cumulative Fe load is the sum of all Fe that was loaded into the PG stream without subtraction of Fe loss from zones where Fe was attenuated. Hence, comparison of the cumulative Fe load to the sampled Fe load provides a good indication of the extent of Fe loss in PG (e.g., Kimball et al., 2002). Fig. 6 presents the exact same information for Zn. Several zones in PG were identified where distinctive changes in the Fe and/or Zn loads occurred. The starts of these zones are demarcated with solid lines and are labeled 1 through 5 in Figs. 2–6. Representative pictures of these zones are included in online supplemental Fig. 1S. Fig. 7 is a ternary diagram where stream and well-water samples are plotted in Al, Mg and Fe space. The stream water samples labeled as Zones 1–5 were collected in these discrete reaches, and the stream samples collected between these discrete zones fall in sequence along the dashed curves that represent mixing or metal attenuation pathways.

The $\delta^{56}$Fe and $\delta^{66}$Zn of filtered groundwater samples from all monitoring wells sampled averaged −0.17 ± 0.16‰ (1$\sigma$; $n$ = 4 wells) and +0.16 ± 0.08‰ (1$\sigma$; $n$ = 5 wells), respectively. The $\delta^{56}$Fe and $\delta^{66}$Zn of the tested QSP-altered rock was 0.11 ± 0.15‰ (2$\sigma$; $n$ = 2) and 0.11 ± 0.08‰ (2$\sigma$; $n$ = 3), respectively. These data and isotopic data for the tested unfiltered and ultrafiltered samples are presented in Table 1S.

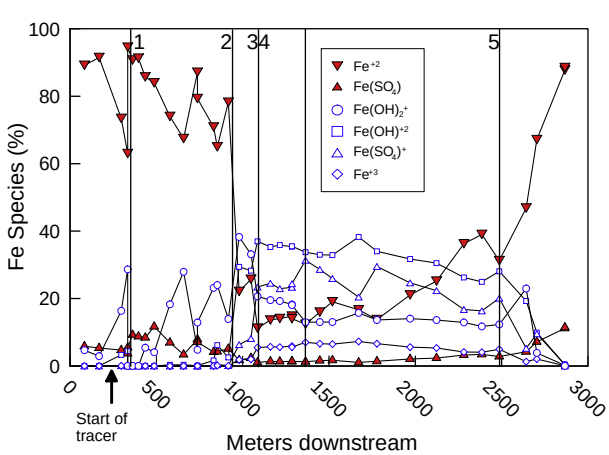


**Fig. 4.** Equilibrium speciation of dissolved Fe calculated using PHREEQC. Numbers 1–5 and the associated lines denote locations of Fe or Zn loading discussed in the text.

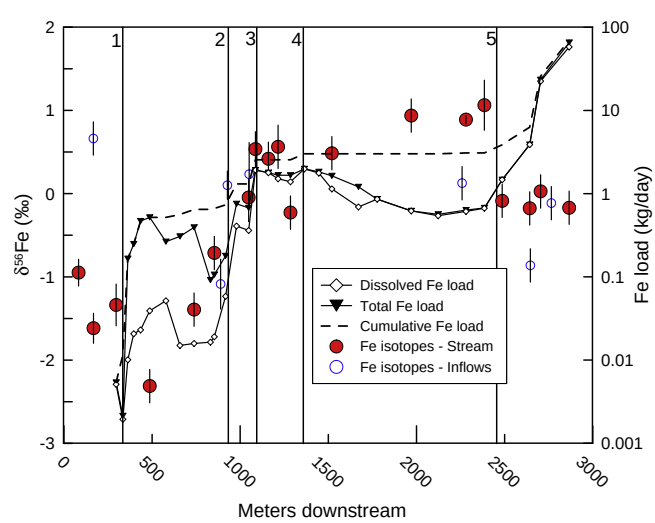


**Fig. 5.** Dissolved, total, and cumulative Fe loads (kg/day) in Prospect Gulch and the Fe isotopic composition of selected filtered stream and inflow samples. Zones of metal loading are presented as solid lines labeled 1–5. Error bars are 2$\sigma$ uncertainties based on repeated measurements.

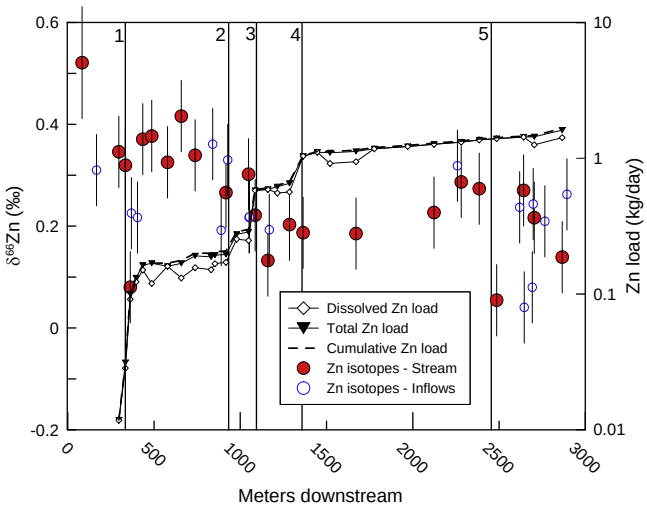


**Fig. 6.** Dissolved, total, and cumulative Zn loads (kg/day) in Prospect Gulch and the Zn isotopic composition of selected filtered stream and inflow samples. Zones of metal loading are presented as solid lines labeled 1–5. Error bars are 2$\sigma$ uncertainties based on repeated measurements.

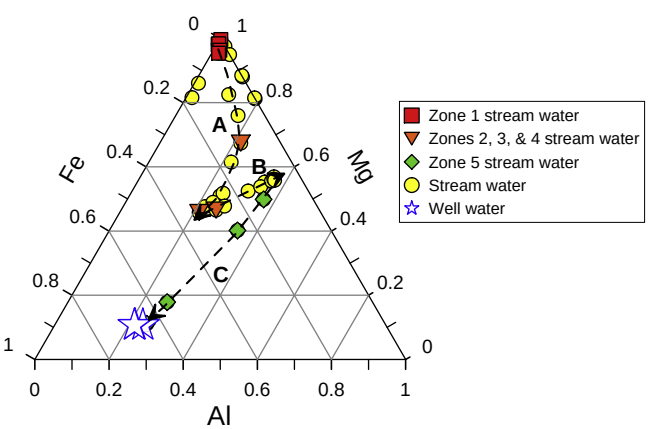


**Fig. 7.** Ternary plot of stream and well-water samples in Al, Mg and Fe space. Stream water samples labeled as Zones 1–5 were collected in discrete narrow reaches of the stream where metal loads increased (these zones are further defined in the text). The stream samples collected between these discrete zones fall in sequence along the dashed curves. The chemical relationships highlighted by these dashed curves are as follows: (A) Mixing of Zone 1 with Zones 2 followed by 3 and 4; (B) Attenuation of Fe between Zones 4 and 5; (C) Mixing of stream water with groundwater (star symbols) in Zone 5.

## 5. Discussion

The approach to this investigation was to first use the tracer dilution and bulk geochemical data to identify reaches in the PG stream where metal loading or in-stream geochemical processes were occurring. The Fe and Zn isotopic data were then used to help identify metal sources and loading/attenuation mechanisms in these reaches. Iron and Zn isotopes were specifically chosen for this investigation because of the inherent differences in how each element is likely to be fractionated in stream waters. For example, Fe isotopes in PG are likely to be affected by redox transformations associated with weathering reactions and precipitation of Fe(III)-oxide minerals. Conversely, Zn isotopes are not subject to redox-related transformations and are likely to behave conservatively under the low pH conditions in PG. It is suspected that different anthropogenic and natural metal sources may have distinctive Fe and Zn isotopic signatures because (1) anthropogenic sources like mine wastes are likely to contain more and possibly different Fe and Zn-bearing minerals (i.e., ore or gangue material) than would be found in host rocks, and (2) the weathering rates of exposed sulfide minerals are likely to be significantly greater in waste rock piles than in the host rock. Differences in the rates of weathering could impact the degree of isotopic fractionation during incongruent dissolution of Fe and Zn-bearing minerals (e.g., Beard and Johnson, 2004). Below, we highlight 5 zones of metal loading and one zone where Fe is strongly attenuated in PG. In this discussion, stream locations are identified by their distance downstream from the point at which the tracer was injected into the stream.

### 5.1. Zone 1

Zone 1, in the upper reaches of the stream (342–500 m) is characterized by its near-neutral pH (Fig. 2), its distinctly light dissolved $\delta^{56}$Fe (<−2.0‰; Fig. 5), and its distinctly heavy $\delta^{66}$Zn (>+0.4‰; Fig. 6). Maximum Fe and Zn loads in Zone 1 are 0.52 and 0.17 kg/day, respectively (Figs. 5 and 6). The stream chemistry in Zone 1 is dominated by Fe-rich anoxic groundwater draining from a fen. Flow from the fen increases the total stream flow in PG by more than five times (see LiBr dilution in Fig. 3a and Table 1S). Iron(II) species are dominant in Zone 1 (Fig. 4), and Fe(II) concentrations in pore waters in the fen (sampled the following year using a vacuum-sealed soil lysimeter apparatus) ranged from 1.1 mg/L at 5 cm depth to >20 mg/L at 60 cm depth.

Suspended Fe(III)-minerals in Zone 1 represent 90–96% of the total Fe load (Fig. 5). The $\delta^{56}$Fe of two unfiltered acidified samples (i.e., suspended + dissolved Fe) from Zone 1 were +0.04‰ and +0.11‰ (Table 1S). Because of the abundance of suspended Fe in Zone 1, the heavier $\delta^{56}$Fe of this load offsets through isotopic mass balance the very light $\delta^{56}$Fe of the dissolved phase. The "overall" (i.e., suspended + dissolved) $\delta^{56}$Fe of these waters matches well with the $\delta^{56}$Fe of groundwater from sampled monitoring wells and with the $\delta^{56}$Fe of groundwater infiltration measured in Zone 5 (see Section 5.4). Additional testing demonstrated that the $\delta^{56}$Fe of an ultra-filtered (<0.001 μm) sample was the same as that measured in an aliquot of the same sample filtered using a 0.45 μm membrane, suggesting that Fe colloids did not control the dissolved metal isotopic signature of PG (Table 1S). Note that the inflow sample at 167 m downstream has a heavier $\delta^{56}$Fe than the filtered stream water samples in Zone 1. The 167 m inflow is small (0.2L/s), does not drain the fen, and has the same characteristics as stream and inflow samples further downstream, including a low pH (3.3) and a low suspended Fe load (see Section 5.2).

The light $\delta^{56}$Fe of the dissolved phase in Zone 1 is consistent with the oxidation of Fe(II) to Fe(III) and the precipitation of Fe(III)-oxides. Under circumneutral pH conditions, $Fe(II)_{aq}$ will rapidly oxidize to $Fe(III)_{aq}$ in the presence of atmospheric $O_2$ (e.g., Nordstrom and Southam, 1997). Isotopic equilibrium between reduced and oxidized aqueous Fe species (e.g., $[Fe^{II}(H_2O)_6]^{+2}$ and $[Fe^{III}(H_2O)_6]^{+3}$) occurs rapidly with the oxidized species incorporating the heavier Fe isotopes ($\Delta^{56}Fe_{Fe(III)aq\text{-}Fe(II)aq} \cong +3.0‰$; Welch et al., 2003; Anbar et al., 2005). Under neutral pH conditions, the isotopically heavy $Fe(III)_{aq}$ is quickly precipitated as ferrihydrite, and this 2-step process of equilibrium of oxidized and reduced Fe species in solution followed by precipitation of Fe(III)-oxides has been shown experimentally and in field studies to drive the $\delta^{56}$Fe of dissolved Fe to light values (e.g., Bullen et al., 2001; Beard and Johnson, 2004; Herbert and Schippers, 2008; Fernandez and Borrok, 2009). The elevated pH and large suspended Fe loads in Zone 1 provide strong evidence that abiotic precipitation is the controlling mechanism. However, additional abiotic or biologic processes can also impact the $\delta^{56}$Fe of the dissolved phase. For example, adsorption of Fe(II) onto mineral surfaces could drive dissolved Fe to a lighter $\delta^{56}$Fe through preferential adsorption of the

heavy Fe isotopes (e.g., Beard et al., 2003; Icopini et al., 2004). Moreover, leaching of Fe with dissolved organic ligands (like those found in soils) has been shown to prefer the lighter Fe isotopes (Brantley et al., 2001). Finally, dissimilatory reduction of Fe(III)-oxides within anoxic soils has been shown to produce extremely light Fe isotopes in soil/sediment pore waters (e.g., Crosby et al., 2007). Additional spatially-detailed testing of the waters, soils, and microbes in Zone 1 would be necessary to quantify the possible impact of these complimentary biogeochemical reactions.

The suspended load for Zn in Zone 1 comprised less than 21% of the total Zn in all samples (Fig. 6). This demonstrates that adsorption of Zn onto Fe(III)-oxide phases was limited. Balistrieri et al. (2008) experimentally constrained a separation factor for Zn adsorption onto ferrihydrite of +0.53‰ ($\Delta^{66}Zn_{adsorbed\text{-}solution}$), which was later confirmed by Juillot et al. (2008). Isotopic mass balance calculations using this separation factor suggest that more than 20% adsorption of Zn would be needed for a difference in the $\delta^{66}$Zn of unfiltered versus filtered stream samples to be measured. This explains why the tested pair of raw vs. filtered stream samples were isotopically indistinguishable (Table 1S). Moreover, if surface adsorption of Zn were an important part of the PG system it would drive the $\delta^{66}$Zn of the dissolved phase to lighter values, which is not what was observed (Fig. 6). It is suspected that the reason why the $\delta^{66}$Zn in Zone 1 was enriched in the heavy Zn isotopes is that much of the free Zn derived from the fen environment was complexed with dissolved organic matter. It has been shown that Zn-organic complexes with dissolved humic acids (Jouvin et al., submitted for publication) or with organic-acid functional groups on microbial surfaces are isotopically heavy in comparison to free $Zn^{+2}$ (Gélabert et al., 2006; John et al., 2007; Borrok et al., 2008b). The flushing of organically-complexed Zn through the fen environment is an explanation that fits the data, but is certainly one that requires further testing to fully evaluate. An alternate explanation is that the host rock/soil itself in Zone 1 is distinct and possesses a uniquely heavy $\delta^{66}$Zn compared to the rest of the rock in the PG.

### 5.2. Zones 2, 3, and 4

Zones 2, 3, and 4 (~950–1364 m) are rich in protons and metals, including Fe and Zn, largely derived from a series of acidic inflows that drain anthropogenic sources, including abandoned mines and sulfide-rich waste-rock piles (Figs. 2, 5 and 6). Iron and Zn loads increase to 1.99 and 1.04 kg/day, respectively, by the end of Zone 4 (1364 m downstream). The concentrations of Fe, Cu, Pb, Zn and $SO_4$ all increase over this interval while the concentrations of Ca, Mg, Na and K remain relatively stable (Fig. 3). $Iron(III)_{aq}$ species become dominant over $Fe(II)_{aq}$ species in Zones 2–4 (Fig. 4), and almost all the Fe is dissolved (i.e., the Fe concentration in the filtered sample is approximately equal to the Fe concentration in the unfiltered sample). The dashed curve labeled "A" in Fig. 7 illustrates the pathway of chemical mixing of stream waters from Zone 1 with Zone 2 followed by Zones 3 and 4. The evolution of the stream water composition involves the loss of Mg (relative to Fe and Al) and a large increase in the amount of Fe near Zones 3 and 4.

The $\delta^{56}$Fe of dissolved stream water in Zones 2–4 ranges from ~0 to +0.6‰, which matches well with the $\delta^{56}$Fe of the bulk (suspended + dissolved) Fe load in Zone 1 (see discussion above). The $\delta^{56}$Fe of Zones 2–4 also matches well with the $\delta^{56}$Fe of the leachate from weathering experiments with QSP-altered rock from PG performed by Fernandez and Borrok (2009). These experiments demonstrate that oxidation of the pyrite surface can result in an easily-leachable layer that is enriched in the heavier Fe isotopes. Although this layer is quickly leached away in experiments, it may be one explanation for the range of $\delta^{56}$Fe observed. Precipitation of Fe(III)-oxides in Zones 2–4 may additionally impact the $\delta^{56}$Fe of PG (see discussion of Zone 5 below); however, under acidic conditions, adsorption reactions are not expected to significantly impact Fe or Zn isotopes.

The $\delta^{66}$Zn in dissolved stream water in Zones 2–4 becomes lighter compared to Zone 1 and approaches the $\delta^{66}$Zn of the sampled QSP rock from PG (Fig. 6). Assuming Zn isotopes are not fractionated significantly during weathering processes (an idea supported by recent experimentation by Fernandez and Borrok, 2009), this change is best explained by mixing of isotopically distinct Zn from Zone 1 with Zones 2–4. To a first approximation the cumulative Zn load is the same as the instantaneous Zn load throughout PG (Fig. 6), suggesting that Zn is behaving conservatively. Because Zone 1 has a small load of Zn in comparison to Zones 2–4 (Fig. 6), the heavy $\delta^{66}$Zn signature from Zone 1 is quickly lost.

### 5.3. Zones of Fe attenuation

Zones of Fe loading in PG are interrupted by stream reaches where the Fe load decreases. The difference between the cumulative Fe load (Fig. 5) and the instantaneous Fe load in the stream at any given point (Fig. 5) is a good approximation of the amount of Fe that has been lost to precipitation in PG. For example, the largest amount of the total Fe load in PG is lost between Zones 4 (1364 M downstream) and 5 (2385 M downstream; Fig. 5). This attenuation corresponds to a steady increase in the $\delta^{56}$Fe of the stream water from ~+0.5‰ at Zones 2–4 to ~+1.1‰ prior to Zone 5. The loss of Fe over this stretch does not appear to be caused by dilution, as the concentrations of other elements like Cu, Pb, Al and Zn were not diluted over this interval (Fig. 3a), suggesting that the mechanism of attenuation was specific to Fe. Moreover, if the loss of Fe was attributable only to dilution from non-Fe bearing waters, the $\delta^{56}$Fe of the stream would not change. Hence, the loss of Fe is most likely attributable to the precipitation of Fe(III)-oxide minerals in the stream channel and/or within the hyporehic zone. Ferricrete coats the stream bed over this interval, supporting the interpretation. This trend of Fe attenuation is illustrated as a dashed line labeled "B" in the ternary diagram, Fig. 7. Note that the relative proportions of Mg and Al remain constant while only Fe is lost.

Rapid precipitation of Fe(III)-oxides via the hydrolysis pathway (i.e., from an over-saturated Fe(III)-rich solution) has been shown to impart a kinetic isotopic fractionation where the lighter isotopes of Fe are preferentially incorporated into the mineral phase (Skulan et al., 2002; Balci et al., 2006). Skulan et al. (2002) have shown that Fe(III) incorporation into an Fe(III)-mineral under less-rapid conditions (i.e., approaching equilibrium) does not significantly impact the Fe isotopic composition. Note that the precipitation of $Fe(III)_{aq}$ via hydrolysis is not the same as the precipitation pathway in Zone 1 where $Fe(II)_{aq}$ was oxidized to $Fe(III)_{aq}$ before forming a precipitate. In Zone 1 the large Fe isotope fractionation was produced through this initial redox step in aqueous solution and was only secondarily affected by the precipitation process. In the reach between Zones 4 and 5, $Fe(III)_{aq}$ species are more abundant than $Fe(II)_{aq}$ species, and oxidation of $Fe(II)_{aq}$ to $Fe(III)_{aq}$ is kinetically prohibited because of the acidic pH conditions (Nordstrom and Southam, 1997). Geochemical modeling using PHREEQC indicates that several Fe(III)-minerals, including ferrihydrite, goethite, and jarosite are over-saturated over part or all of the interval where Fe is attenuated.

The $\delta^{66}$Zn of PG becomes slightly heavier compared to Zones 2–4 starting around 2200 m downstream (Fig. 6). Unlike Fe, the Zn load increases by 0.33 kg/day over this stretch (Fig. 6). The cumulative in-stream Zn load is almost indistinguishable from the instantaneous total Zn load at every point (Fig. 6), demonstrating that Zn is not attenuated in PG. This additional Zn must be

isotopically heavier than the Zn in Zones 2–4 to increase the $\delta^{66}$Zn of the stream. It is suspected that this Zn is contributed by diffuse seeps from soil and vegetation along the stream walls, as no discrete inflows were identified for sampling.

### 5.4. Zone 5

Zone 5 (~2400 m to the mouth of PG) is characterized by an abrupt change in $\delta^{56}$Fe from +1.1‰ upstream of Zone 4 to −0.1‰ downstream (Fig. 5). This isotopic change correlates with a two orders of magnitude or more increase in Fe load to ~65 kg/day (Fig. 5) and significant increases in the concentrations of Al, $SO_4$, K and Mg (Fig. 3). Despite this dramatic change in Fe load, the pH of PG remains invariant (Fig. 2). The total Zn load increases only slightly in Zone 5 to a maximum of 1.61 kg/day (Fig. 6), and the $\delta^{66}$Zn of the stream water and inflows to PG fluctuates from ~+0.05 to +0.25‰.

Diffuse inflows of water from the stream walls, Fe-rich springs adjacent to the stream, and a sharp increase in Fe(II) species in the stream (Fig. 4) all suggest that groundwater is infiltrating the stream channel in Zone 5. Nearby flowing artesian wells confirm that the hydraulic head for deep groundwater near the mouth of PG is above the present-day land surface. Apparent $^3$H/He age dates of the groundwater from these wells are dominantly 5–30 years (Johnson et al., 2007).

Fig. 7 provides evidence of chemical mixing (dashed line labeled "C") between the stream and Fe-rich groundwater. The chemical composition of samples from the three monitoring wells nearest to the mouth of PG (screened at depths of 7.5 m, 24.7 m, and 39 m; see Johnson and Yager, 2006) are presented as stars to represent the end-member groundwater component (Fig. 7). Mixing of groundwater with surface water involves a large increase in the flux of Fe to the stream and a significant loss in Mg relative to Al (Fig. 7). The $\delta^{56}$Fe of the upwelling groundwater in Zone 5 is most likely a direct reflection of the Fe isotopic composition of the groundwater, and because of the low pH the $\delta^{56}$Fe is not additionally impacted by redox interactions or chemical processes like adsorption or precipitation. Moreover, the oxidation of $Fe(II)_{aq}$ to $Fe(III)_{aq}$ is kinetically prohibited below pH 4.0 (e.g., Nordstrom and Southam, 1997).

In an earlier investigation, Borrok et al. (2008a) reported $\delta^{66}$Zn measurements for filtered water samples collected over a 24-h period from Zone 5. The $\delta^{66}$Zn of the stream was invariant with time and averaged +0.4‰. This average is ~0.15‰ heavier than the data reported for Zone 5 in the current investigation. The reason for this difference is unclear; however, it could be the result of long-term or seasonal variability in $\delta^{66}$Zn in PG. The samples reported by Borrok et al. (2008a) were collected under different flow conditions 2 years before the current investigation.

## 6. Conclusions

In this investigation Fe and Zn isotopes were used with additional hydrologic and geochemical constraints to distinguish metal sources and attenuation mechanisms in an alpine watershed. In this single alpine catchment the $\delta^{56}$Fe and $\delta^{66}$Zn of filtered stream water samples varied by ~3.5‰ and 0.4‰, respectively (about 70% and 25% of their respective variation in natural samples). Most of the variation in $\delta^{56}$Fe occurred during redox interactions and mineral precipitation processes. For example, rapid oxidation of Fe(II) entering the stream from a fen led to precipitation of isotopically heavy Fe(III)-oxides, which imparted a distinctively light $\delta^{56}$Fe to the remaining dissolved Fe in the stream water. In-stream geochemical processes did not impact the $\delta^{66}$Zn of filtered stream waters. Instead, changes in $\delta^{66}$Zn could largely be attributed to conservative mixing of isotopically distinct sources. For example, waters from the fen ($\delta^{66}$Zn ~ +0.4‰) were mixed with lighter Zn isotopes ($\delta^{66}$Zn ~ +0.2‰) from mining waste piles further downstream It is speculated that the heavy $\delta^{66}$Zn of the fen may be attributable to complexation with dissolved organic matter, but this hypothesis needs further testing.

This initial investigation of a mountain watershed suggests that Fe and Zn isotopes may prove useful for (1) helping to distinguish between anthropogenic and natural metal loading sources, (2) pinpointing the contributions to metal loading from fens or wetlands, (3) establishing chemical links between groundwater and surface water, and (4) understanding in-stream geochemical processes that impact metal transport. As insights continue to be gained on the fractionation behaviors of these metals in complex systems, it is anticipated that they will become more common as geochemical probes for similar investigations.

## Acknowledgments

This work was supported by the US Geological Survey's (USGS) Mineral and Crustal Resources Programs, Mendenhall Post-Doctoral Fellowship Program (for Borrok), and Toxic Substances Hydrology Program. We thank Katie Walton-Day, David Nimick, Ray Johnson, George Breit, Monique Adams, and Ruth Wolf for providing assistance with field sampling and/or laboratory analysis. Tom Bullen and Andy Manning provided helpful feedback on early drafts of the manuscript. The manuscript also benefited greatly from the input of two anonymous reviewers, and a thorough review provided by the Editor, Ron Fuge. The use of firm, trade, or brand names in this paper is for identification purposes only and does not constitute endorsement by the USGS.

## Appendix A. Supplementary material

Supplementary material associated with this article can be found, in the online version, at doi:10.1016/j.apgeochem.2009.03.010.

## References

Anbar, A.D., Jarzecki, A.A., Spiro, T.G., 2005. Theoretical investigation of iron isotope fractionation between $Fe(H_2O)_6^{3+}$ and $Fe(H_2O)_6^{2+}$: implications for iron stable isotope geochemistry. Geochim. Cosmochim. Acta 69, 825–837.

Balci, N., Bullen, T.D., Witte-Lien, K., Shanks, W.C., Motelica, M., Mandernack, K.W., 2006. Iron isotope fractionation during microbially simulated Fe(II) oxidation and Fe(III) precipitation. Geochim. Cosmochim. Acta 70, 622–639.

Bales, R.C., Molotch, N.P., Painter, T.H., Dettinger, M.D., Rice, R., Dozier, J., 2006. Mountain hydrology of the western United States. Water Resour. Res. 42, W08432. doi:10.1029/2005WR004387.

Balistrieri, L.S., Borrok, D.M., Wanty, R.B., Ridley, W.I., 2008. Fractionation of Cu and Zn isotopes during adsorption onto amorphous Fe(III) oxides: experimental mixing of acid rock drainage and pristine river water. Geochim. Cosmochim. Acta 72, 311–328.

Beard, B.L., Johnson, C.M., 2004. Fe isotopic variations in the modern and ancient Earth and other planetary bodies. Rev. Min. Geochem. 55, 319–357.

Beard, B.L., Johnson, C.M., Von Damm, K., Poulson, R., 2003. Iron isotope constraints on Fe cycling and mass balance in oxygenated Earth Oceans. Geology 31, 629–632.

Bergquist, B.A., Boyle, E.A., 2006. Iron isotopes in the Amazon River system: weathering and transport signatures. Earth Planet. Sci. Lett. 248, 54–68.

Borrok, D.M., Nimick, D.A., Wanty, R.B., Ridley, W.I., 2008a. Isotopic variations of dissolved copper and zinc in stream waters affected by historical mining. Geochim. Cosmochim. Acta 72, 329–344.

Borrok, D.M., Ridley, W.I., Wanty, R.B., 2008b. Isotopic fractionation of Cu and Zn during adsorption onto bacterial surfaces. Goldschmidt Conf. (abstract A99).

Borrok, D.M., Wanty, R.B., Ridley, W.I., Wolf, R., Lamothe, P.J., Adams, M., 2007. Separation of copper, iron, and zinc from complex aqueous solutions for isotopic measurement. Chem. Geol. 242, 400–414.

Bove, D.J., Mast, M.A., Dalton, J.B., Wright, W.G., Yager, D.B., 2007. Major styles of mineralization and hydrothermal alteration and related solid- and aqueous-phase geochemical signatures. In: Church, S.E., von Guerard, P., Finger, S.E. (Eds.), Integrated Investigations of Environmental Effects of Historical Mining in

the Animas River Watershed, San Juan County, Colorado. US Geol. Surv. Prof. Paper 1651.
Bove, D.J., Mast, M.A., Wright, W.G., Verplanck, P.L., Meeker, G.P., Yager, D.B., 2000. Geologic control on acidic and metal-rich waters in the southeast Red Mountains area, near Silverton, Colorado. In: Proc. 5th Internat. Conf. Acid Rock Drainage. Society for Mining and Metallurgy, and Exploration, Inc., pp. 523–533.
Brantley, S.L., Liermann, L., Bullen, T.D., 2001. Fractionation of Fe isotopes by soil microbes and organic acids. Geology 29, 535–538.
Brinton, T.I., Antweiler, R.C., Taylor H.E., 1995. Method for the determination of dissolved chloride, nitrate, and sulfate in natural water using ion chromatography. US Geol. Surv. Open-File Rep. 95-426A.
Brooks, P.D., McKnight, D.M., Bencala, K.E., 2001. Annual maxima in Zn concentrations during spring snowmelt in streams impacted by mine drainage. Environ. Geol. 40, 1447–1454.
Bullen, T.D., White, A.F., Childs, C.W., Vivit, D.V., Schulz, M.S., 2001. Demonstration of a significant abiotic iron isotope fractionation in nature. Geology 29, 699–702.
Chapman, B.M., Jones, D.R., Jung, R.F., 1983. Processes controlling metal ion attenuation in acid mine drainage streams. Geochem. Cosmochim. Acta 47, 1957–1973.
Chen, J., Gaillardet, J., Louvat, P., 2008. Zn isotopes in the Seine River Waters, France: a probe of anthropogenic contamination. Environ. Sci. Technol. 42, 6494–6501.
Cloquet, C., Cariganan, J., Libourel, G., 2006. Isotopic composition of Zn and Pb atmospheric depositions in an urban/periurban area of Northeastern France. Environ. Sci. Technol. 40, 6594–6600.
Crosby, H.A., Roden, E.E., Johnson, C.M., Beard, B.L., 2007. The mechanisms of iron isotope fractionation produced during dissimilatory Fe(III) reduction by Shewanella putrefaciens and Geobacter sulfurreducens. Geobiology 5, 169–189.
Emmanuel, S., Erel, Y., Mathews, A., Teutsch, N., 2005. A preliminary mixing model for Fe isotopes in soils. Chem. Geol. 222, 23–34.
Fantle, M.S., DePaolo, D.J., 2004. Iron isotopic fractionation during continental weathering. Earth Planet. Sci. Lett. 288, 547–562.
Fernandez, A., Borrok, D.M., 2009. Fractionation of Cu, Fe, and Zn isotopes during the oxidative weathering of sulfide-rich rocks. Chem. Geol. doi:10.1016/j.chemgeo.2009.01.024.
Gélabert, A., Pokrovsky, O.S., Viers, J., Schott, J., Boudou, A., Feurtet-Mazel, A., 2006. Interaction between zinc and freshwater and marine diatom species: surface complexation and Zn isotope fractionation. Geochim. Cosmochim. Acta 70, 839–857.
Herbert, R.B., Schippers, A., 2008. Iron isotope fractionation by biogeochemical processes in mine tailings. Environ. Sci. Technol. 42, 1117–1122.
Icopini, G.A., Anbar, A.D., Ruebush, S.S., Tien, M., Brantley, S.L., 2004. Iron isotope fractionation during microbial reduction of iron: the importance of adsorption. Geology 32, 205–208.
Ingri, J., Malinovsy, D., Rodushkin, I., Baxter, D.C., Widerlund, A., Andersson, P., Gustafsson, O., Forsling, W., Öhlander, B., 2006. Iron isotope fractionation in river colloidal matter. Earth Planet. Sci. Lett. 245, 792–798.
John, S.G., Geis, R.W., Saito, M.A., Boyle, E.A., 2007. Zinc isotope fractionation during high-affinity and low-affinity zinc transport by the marine diatom *Thalassiosira oceanica*. Limnol. Oceanog. 52, 2710–2714.
Johnson, D.B., Hallberg, K.B., 2005. Acid mine drainage remediation options. A review. Sci. Total Environ. 338, 3–14.
Johnson, R.H., Yager, D.B., 2006. Completion reports, core logs, and hydrogeologic data from wells and piezometers in Prospect Gulch, San Juan County, Colorado. US Geol. Surv. Open-File Rep. 2006-1030.
Johnson, R.H., Wirt, L., Manning, A.H., Leib, K.J., Fey, D.L., Yager, D.B., 2007. Geochemistry of surface and ground water in Cement Creek from Gladstone to Georgia Gulch and in Prospect Gulch, San Juan County, Colorado. US Geol. Surv. Open-File Rep. 2007-1004.
Jouvin, D., Louvat, P., Juillot, F., Maréchal, C.N., Benedetti, M.F., submitted for publication. Zn isotopic fractionation: why organic matters. Environ. Sci. Technol.
Juillot, F., Marechal, C., Ponthieu, M., Cacaly, S., Morin, G., Benedetti, M., Hazemann, J.L., Proux, O., Guyot, F., 2008. Zn isotopic fractionation caused by sorption on goethite and 2-Lines ferrihydrite. Geochim. Cosmochim. Acta 72, 4886–4900.
Kimball, B.A., Runkel, R.L., Walton-Day, K., Bencala, K.E., 2002. Assessment of metal loads in watersheds affected by acid mine drainage by using tracer injection and synoptic sampling: cement creek, Colorado, USA. Appl. Geochem. 17, 1183–1207.
Kimball, B.A., Walton-Day, K., Runkel, R.L., 2007. Quantification of metal loading by tracer injection and synoptic sampling, 1996–2000. In US Geol. Surv. Prof. Paper 1651 (Chapter E9).
Lamothe, P.J., Meier, A., Wilson, S., 2002. The determination of forty-four elements in aqueous samples by inductively coupled plasma, mass spectrometry. US Geol. Surv. Open-File Rep. 02-0223.
Lipman, P.W., Fisher, F.S., Mehnert, H.H., Naeser, C.W., Luedke, R.G., Steven, T.A., 1976. Multiple ages of mid-Tertiary mineralization and alteration in the western San Juan Mountains. Colorado. Econ. Geol. 71, 571–588.
Nordstrom, D.K., Southam, G., 1997. Geomicrobiology of sulfide mineral oxidation. Rev. Mineral. Geochem. 35, 361–390.
Parkhurst, D.L., Appelo, C.A.J., 1999. User's guide to PHREEQC (Version 2) - A computer program for speciation, batch-reaction, one-dimensional transport, and inverse geochemical calculations. US Geol. Surv. Water Resour. Invest. Rep. 99-4259.
Petit, J.C.J., de Jong, J., Chou, L., Mattielli, N., 2008. Development of Cu and Zn isotope MC-ICP-MS measurements: applications to suspended particulate matter and sediments from the Scheldt Estuary. Geostand. Geoanal. Res. 32, 149–166.
Pokrovsky, O.S., Viers, J., Freydier, R., 2005. Zinc stable isotope fractionation during its adsorption on oxides and hydroxides. J. Colloid Interface Sci. 291, 192–200.
Runkel, R.L., Kimball, B.A., 2002. Evaluating remedial alternatives for an acid mine drainage stream: application of a reactive transport model. Environ. Sci. Technol. 36, 1093–1101.
Runkel, R.L., Kimball, B.A., Walton-Day, K., Verplanck, P.L., 2007. A simulation-based approach for estimating premining water quality – Red Mountain Creek. Colorado. Appl. Geochem. 22, 1899–1918.
Skulan, J.L., Beard, B.L., Johnson, C.M., 2002. Kinetic and equilibrium Fe isotopic fractionation between aqueous Fe(III) and hematite. Geochim. Cosmochim. Acta 66, 2995–3015.
Sonke, J.E., Sivry, Y., Viers, J., Freydier, R., Dejonghe, L., Andre, L., Aggarwal, J.K., Fontan, F., Dupre, B., 2008. Historical variations in the isotopic composition of atmospheric zinc deposition from a zinc smelter. Chem. Geol. 252, 145–157.
Wanty, R.B., Verplanck, P.L., Tuttle, M.L., Runkel, R.L., Berger, B.R., Kimball, B.A., 2004. Resolving natural and anthropogenic sources of solutes to a watershed from historic mining. In: Wanty, R.B, Seal, II, R.R. (Eds.), Proc. 11th Internat. Symp. Water–Rock Interaction, Balkema, New York, 1659-1663.
Weiss, D.J., Raush, N., Mason, T.F.D., Coles, B.J., Wilkinson, J.J., Ukonmaanaho, L., Arnold, T., Nieminen, T.M., 2007. Atmospheric deposition and isotope biogeochemistry of zinc in ombrotrophic peat. Geochim. Cosmochim. Acta 71, 3498–3517.
Welch, S.A., Beard, B.L., Johnson, C.M., Braterman, P.S., 2003. Kinetic and equilibrium Fe isotope fractionation between aqueous Fe(II) and Fe(III). Geochim. Cosmochim. Acta 67, 4231–4250.
Williams, M.W., Losleben, M.V., Hamann, H.B., 2002. Alpine areas in the Colorado front range as monitors of climate change and ecosystem response. Geograph. Rev. 92, 180–192.